



Precipitation chemistry and stable isotopic characteristics at Wengguo in the northern slopes of the Himalayas

Subash Adhikari, et al. [full author details at the end of the article]

Received: 25 February 2019 / Accepted: 31 January 2020 /
Published online: 18 February 2020
© Springer Nature B.V. 2020

Abstract

The major ions in precipitation can reflect the conditions of the atmosphere, while stable isotopic characteristics provide information on the moisture source. In order to understand the local hydro-chemical features and regional geochemical cycle, it is essential to assess the chemical composition of precipitation and the associated sources. Therefore, a total of 57 precipitation samples (2016 to 2017) for major ions and 178 samples (2013 to 2017) for stable isotopes were collected from the Wengguo station and analyzed to explore the major ionic deposition and stable isotopic characteristics in the northern slopes of the Himalayas. The average pH and electrical conductivity were 6.82 ± 0.45 and $15.36 \pm 11.67 \mu\text{S cm}^{-1}$, respectively. Ca^{2+} followed by K^{+} and Mg^{2+} played a crucial role in neutralizing the precipitation acidity. The major ionic sources in the region were terrigenous (Ca^{2+} , HCO_3^{-} , and Mg^{2+}) and sea salt (Na^{+} , Cl^{-} , and Mg^{2+}), as well as anthropogenic emissions (SO_4^{2-} and NO_3^{-}) and biomass burning (K^{+}). The total deposition flux of the major ions was higher in 2016 than in 2017 and was influenced by the higher precipitation. The average values of $\delta^{18}\text{O}$ and δD in precipitation were $-15.22 \pm 5.17 \text{‰}$ and $-116.01 \pm 41.31 \text{‰}$, respectively. The precipitation stable isotopes were not significantly correlated to the local air temperature but the precipitation amount. Moreover, the variation in stable isotopes, local meteoric water line, and d-excess indicated the existence of continental and monsoon moisture transport systems. The transport of chemicals over the high elevation region from polluted cities in South Asia via moisture originating in the Bay of Bengal and the Arabian Sea was determined based on the source identification, clusters of air mass backward trajectory analysis, and the National Center for Environmental Prediction Final dataset. Thus, the ionic concentrations and stable isotopic characteristics of the precipitation from this study provided a valuable dataset to assess the atmospheric environment in the northern slopes of the Himalayas at Southern Tibetan Plateau.

Keywords Major ions · Stable isotopes · Wet deposition · Southern Tibetan Plateau

Electronic supplementary material The online version of this article (<https://doi.org/10.1007/s10874-020-09399-1>) contains supplementary material, which is available to authorized users.

1 Introduction

Precipitation, as a significant source of freshwater, plays an essential role in removing the soluble components from the atmosphere (Rao et al. 2016) via in-cloud scavenging and below-cloud washout (Kajino and Aikawa 2015). Wet deposition studies have been broadly used for understanding the local hydro-chemical features and regional geochemical cycles as well as evaluating atmospheric pollution for air quality control (Kulshrestha et al. 2003; Mohan 2016; Pu et al. 2016). This assists in distinguishing the relative contribution of plausible natural sources, such as sea salts, soil and mineral dust, and natural forest fires (Xiao 2016), and anthropogenic emission sources, such as fossil fuels, industrial activities, and biomass burning (Xing et al. 2017). Moreover, the isotopic characteristics related to precipitation provide an indication of the relative humidity, evaporation, and temperature in the moisture transport region and can potentially be used to infer the moisture sources (Hughes and Crawford 2013; Qu et al. 2018).

The chemical constituents of precipitation are affected by various types of sources, meteorological circumstances, and topographic features. In general, sea salt ions (Na^+ and Cl^-), crustal ions (Ca^{2+} , Mg^{2+} , and HCO_3^-), and anthropogenic ions (mainly SO_4^{2-} and NO_3^-) are abundant in coastal sites, in inland areas, and in industrial and urbanized sites, respectively (Zhang et al. 2018). In addition, K^+ can be influenced by biomass burning (Tripathee et al. 2014). Studies surrounding the Tibetan Plateau (TP) show that Ca^{2+} , Mg^{2+} , and K^+ originating from the soil and biomass burning are higher in the Indian plain (Rao et al. 2016)., SO_4^{2-} and NO_3^- resulting from the oxidation of SO_2 and NO_x produced from stationary (coal burning, brick kiln, thermal power plant, and oil refining) and mobile sources (motor vehicles) are higher in the densely populated Indo-Gangetic Plain (IGP) in India (Tiwari et al. 2016) and Bangladesh (Sarin et al. 2010). In the case of the TP, higher crustal ions result from local dust and NO_3^- produced from anthropogenic activities; for instance, dung combustion for heating and cooking (Zhang et al. 2012). The concentration of crustal (Ca^{2+} and Mg^{2+}) and anthropogenic (SO_4^{2-} and NO_3^-) ions is higher in Muztagh Ata, which is located in the drier westerly domain than in Southeast Tibet, which is located in the wetter monsoon domain (Liu et al. 2015). Na^+ and Cl^- in mountainous regions can be influenced by long-range transport (Roy et al. 2016) or extensive convective precipitation (Li et al. 2007). K^+ is influenced by lake evaporation and mineral aerosols and is also a fine tracer of biomass burning (Liu et al. 2013). Monsoon atmospheric circulation may transport significant chemicals from South Asia, thus disturbing the high altitude pristine region through long-range transport (Cong et al. 2010). Therefore, the major ionic composition, nature, and sources from the lowlands to high-altitude regions are distinctly diverse.

The TP is the highest and most extensive mountain region in the world, with an average elevation higher than 4000 m above mean sea level and a total area around $2.5 \times 10^6 \text{ km}^2$. The region has an enormous impact on global and regional climate (Kang et al. 2010a; Yao et al. 2013). The climate of the TP is influenced by the Indian monsoon, the East Asian monsoon, and westerlies (Yao et al. 2013). During the summer monsoon period, the air mass trajectories reaching the TP generally originate from the Arabian Sea and the Bay of Bengal (Tian et al. 2001a), which transfer moisture and dust from areas upwind (Zhang et al. 2014). Several previous studies were performed on the precipitation chemistry in the pristine TP (Kang et al. 2010a; Yao et al. 2012). Zhang et al. (2014) reported the chemical characteristics of precipitation at Lijiang, southeast TP, with Ca^{2+} and HCO_3^- as the dominant cation and anion, respectively and specified the monsoon transportation from the Bay of Bengal. Precipitation chemistry from Nam Co, central TP, revealed that crustal aerosol was responsible for high

loadings of Ca^{2+} , Mg^{2+} , SO_4^{2-} , and HCO_3^- whereas K^+ and Cl^- were influenced by the lake salt and dry lake sediments (Zhang et al. 2012). Similar temporal variation of precipitation chemistry was described in the nearby Zhadang Glaciers (Li et al. 2007). Moreover, the chemical constituents of precipitation in the Qilian Mountain, the northern edge of TP, was SO_4^{2-} - Mg^{2+} - Ca^{2+} type and the major ionic sources were crustal aerosols from central Asia and northwestern arid regions influenced by the westerly and anthropogenic activities (Li et al. 2014). Similarly, a study in northeastern TP also indicated that the concentration of Ca^{2+} was associated with the air mass from the west (Wang et al. 2019).

Numerous researchers have examined the rainwater of urban, rural, and coastal areas from various parts of the world to determine the chemical composition, which may assist in understanding the relative significance of the different contributing sources. Some studies have focused on precipitation chemistry in the southern side of the Himalayas (Tripathee et al. 2014; Tiwari et al. 2016; Khan et al. 2018) and some in the Northern side i.e., TP (Li et al. 2007; Liu et al. 2013; Liu et al. 2015). However, very few studies have evaluated the sources contributing to the chemical composition of precipitation using stable isotopic characteristics. Isotopes are natural tracers that provide information regarding the source of chemicals in water (Huang et al. 2018). The connection between moisture transport trajectory and isotopes in precipitation is illustrated by the direct relationship between the variation in isotopes and moisture origins, and thus isotopic data can potentially be used to infer moisture sources (Qu et al. 2018).

Wengguo in the northern slopes of the Himalayas is located in the monsoon domain at the southern edge of the TP, and the strength of the monsoon directly influences the fluxes of the chemical constituents and stable isotopes in the precipitation. Therefore, the chemical composition of precipitation is also affected by long-range transport. Studying the precipitation chemistry of Wengguo is essential for understanding the existing atmospheric environment and the influence of wet deposition on the local hydrochemistry. The main objectives of this study were to (1) understand the physicochemical characteristics of individual precipitation events during the monsoon season, (2) examine the annual variability in the wet deposition flux of the measured ions, and (3) estimate the contribution of various sources of chemicals and identify the transport pathways revealed by the stable isotopic characteristics. To achieve these objectives, precipitation samples during monsoon season were collected from 2013 to 2017 at Wengguo, northern slopes of the Himalayas in the southern TP for measurement of pH, electrical conductivity, major ions, and stable isotopes. The characteristics and sources of chemical constituents were determined based on enrichment factor, source contribution, correlation analysis, and principal component analysis, etc. Moreover, the moisture sources were revealed by isotopic characteristics, HYSPLIT model, and NCEP FNL datasets.

2 Methodologies

2.1 Site description

The Wengguo hydrological station (90.36° E, 28.90° N, 4569 m above the sea level) is located in the Yamdruk Tso Lake basin, Southern TP (Fig. 1). The mean annual temperature and precipitation as reported by the nearby meteorological station (Langkazi station) are 2.6 °C and 350 mm, respectively (Tian et al. 2008). The relative humidity and temperature during summer are higher, with more than 90% of the annual precipitation relying on the monsoon season,

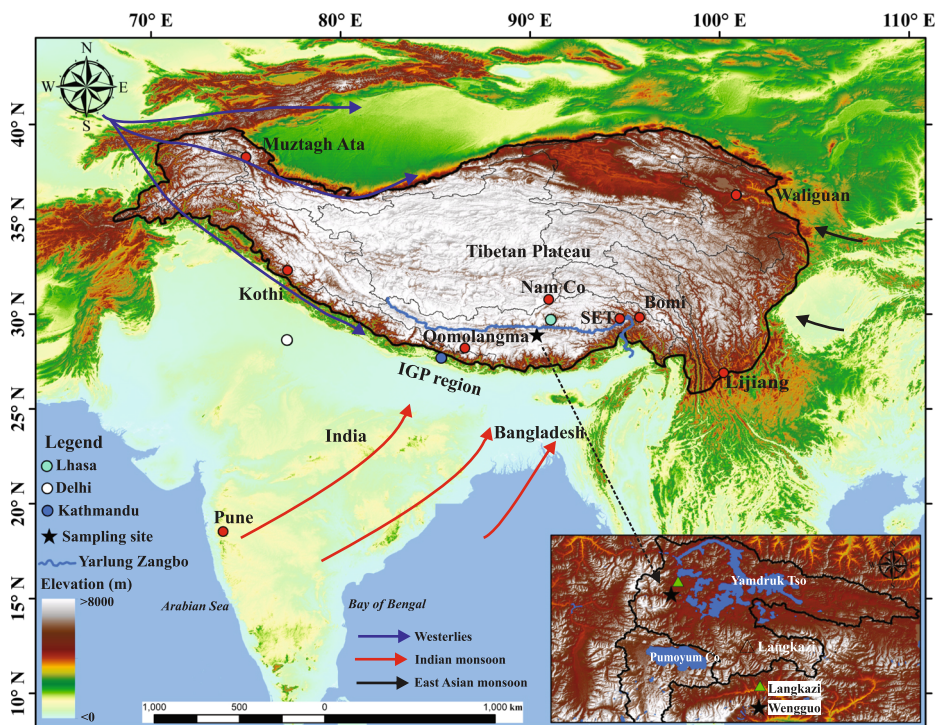


Fig. 1 Location of sampling site in Southern Tibetan Plateau

with the intensity decreasing during the dry season (Fig. S1). The meteorological data were obtained from <http://data.cma.cn/>.

2.2 Sampling and laboratory analysis

A total of 57 event-based precipitation samples for major ions (2016 to 2017) and 178 samples for stable isotopes (2013 to 2017) were collected during the monsoon seasons. Previously washed high-density polyethylene (HDPE) buckets coated internally with changeable HDPE plastic bags were used to collect the samples. All the precipitation samples were poured into HDPE bottles immediately after collection. Before the collection of samples, each of the sampling bottles was washed with nitric acid and ultimately rinsed with deionized water. Furthermore, the sampling bottles were rinsed twice with the same rainwater from the bucket prior to sample collection. The sampling bucket was positioned 1.5 m above the ground to avoid the interaction of soil particles. In each precipitation event, the plastic bag was opened, and the samples were quickly collected to elude interferences due to dry deposition. Electrical conductivity (EC), total dissolved solids (TDS), and pH were measured in situ using a multi-parameter device (HI-98129, HANNA, Romania). Samples for cation analysis were acidified in 2 M HNO_3 . All the samples were preserved in a refrigerator prior to transport to the laboratory of the Institute of Tibetan Plateau Research, Chinese Academy of Sciences (ITP-CAS), Beijing, for chemical analysis. The major cations (Ca^{2+} , Mg^{2+} , K^+ , and Na^+) were evaluated using an Inductively Coupled Plasma Optical Emission Spectrometer (ICP-OES, USA). The anions (Cl^- , NO_3^- , and SO_4^{2-}) were examined by Ion Chromatography (ICS-2500, USA). Because ICP-OES gives elemental instead of ionic concentration, water samples

were filtered through 0.45- μm polytetrafluoroethylene (PTFE) disk syringe filter to reduce uncertainty in ion balance calculation and overestimation of deposition fluxes. The detection limit was 0.01 ppm for both cations and anions. The stable isotopes (δD and $\delta^{18}\text{O}$) were analyzed using a Picarro-L2130i Wave-Scan Cavity Ring-Down Spectrometer with precisions of $\pm 0.15\text{‰}$ for $\delta^{18}\text{O}$ and $\pm 0.5\text{‰}$ for δD . The measured values were expressed as δ ($\delta^{18}\text{O}$ and δD) in parts per million (‰) relative to the Vienna Standard Mean Ocean Water (VSMOW) defined by Gonfiantini (1978) on the basis of the following equation.

$$\delta = \left(\frac{R_{\text{sample}} - R_{\text{VSMOW}}}{R_{\text{VSMOW}}} \right) \times 1000 \quad (1)$$

where R_{sample} stands for the ratio of heavier to lighter isotopes in the water, i.e., D/H for δD and $^{18}\text{O}/^{16}\text{O}$ for $\delta^{18}\text{O}$.

2.3 Data quality control

Special care and precautions were taken during the sampling period and laboratory analysis for quality control. To avoid potential contamination, non-powder vinyl cleanroom gloves were used during all of the activities. Collected samples along with the field blank and replicate samples were stored in the freezer until laboratory analysis to prevent a chemical and biological reaction that could alter the concentration of the ions. Deionized water and freshly prepared standard solutions of known concentration were used during the analysis. Furthermore, the practical blanks were examined during each analytical run to trace the contamination. A set of samples was examined for each calibration curve. The ionic concentration in the field blank was lower than 10% of that in the routine samples. Laboratory blank and duplicate samples experienced negligible contamination during sample collection and transport.

Regression analysis was used to estimate the ionic balance between the anions and cations. The outcome was (Σ anions = 0.63 Σ cations, $R^2 = 0.71$, $p < 0.01$) (Fig. S2), signifying an acceptable data quality. The value of the slope represents the ratio of the sum of anions to the sum of cations, reflecting the anion deficiency due to the exclusion of HCO_3^- (Al-Khashman 2005). Considering the alkaline pH, both in the precipitation and surface soil layer in the TP, the unmeasured anion was likely HCO_3^- (Liu et al. 2015). Due to the lower concentration of organic acids in the region (Liu et al. 2014), the concentration of HCO_3^- was calculated using the charge balance method (Pant et al. 2018). After calculating HCO_3^- , the measured TDS of the rainwater was matched with the total sum of the cations and anions, including HCO_3^- (Σ ions = 1.05 TDS, $R^2 = 0.86$, $p < 0.01$) (Fig. S3), suggesting good data quality (Pant et al. 2018).

2.4 Data analysis

2.4.1 Volume-weighted mean concentration

Event-based samples for the monsoon season were used to explore the average values during the sampling period, and the average ion concentration was reflected as the volume-weighted mean (VWM) (Deusdará et al. 2017), calculated as

$$CA = \frac{\sum(C_i \times P_i)}{\sum(P_i)} \quad (2)$$

where CA represents the volume weight mean concentration in $\mu\text{eq L}^{-1}$, C_i illustrates the ion concentrations of the individual sample ($\mu\text{eq L}^{-1}$), and P_i denotes the precipitation amount (mm) corresponding to each event sample.

2.4.2 Neutralization factor

The neutralizing tendency for any component in precipitation can be conveyed as the neutralization factor (NF) and is calculated using the following formula (Kulshrestha et al. 1995; Tripathee et al. 2014):

$$NF(x) = \frac{(x)}{(NO_3^- + SO_4^{2-})} \quad (3)$$

where X is the ion of interest.

The above calculation was established based on the fact that the major acidifying anions in the atmosphere were SO_4^{2-} and NO_3^- . However, the major neutralizing cations in the precipitation were Ca^{2+} , NH_4^+ , and Mg^{2+} . Na^+ and Cl^- were neglected for the evaluation of NF based on the assumption that they mainly originate from the sea in the form of marine salt.

2.4.3 Source identification of major ions

Statistical analysis With the aim of estimating the association, common variability, and potential sources of the major ions in the precipitation, correlation analysis (CA) and principal component analysis (PCA) were performed. A heatmap based on a bivariate correlation analysis was plotted in R (version 3.5.0, R Foundation for Statistical Computing, Vienna, Austria) using the package pheatmap (Kolde 2019), and the texts in the illustrations were edited using Adobe Illustrator. The PCA was produced using SPSS (version 22.0, IBM Corp., Armonk, NY, USA) for the determination of natural and anthropogenic sources on the chemical composition of precipitation. PCA can extract the perfect configuration of variable loadings in factors with a varimax rotation, which renders the data easier to interpret (Tripathee et al. 2016). The chosen components should have eigenvalues >1 and should explain at least 70 to 80% of the total variance. The initial dimension bears the highest amount of inertia, followed by the second, and so on (Tripathee et al. 2017), in which the relevance of the dataset for PCA/FA was established by applying the Kaiser-Meyer-Olkin (KMO) and Bartlett's sphericity methods.

Enrichment factor (EF) and source contribution Several past studies used the enrichment factor to investigate the source contribution of major ions (Lu et al. 2011; Xiao 2016). For this purpose, Na^+ was used as the reference for seawater considering its predominantly marine origin (Kulshrestha et al. 2003), whereas Ca^{2+} was used as a reference element for the continental crust as its composition in the soil rarely changes (Zhang et al. 2007). Several authors used Na^+ as a sea salt tracer for the source assessment of wet precipitation in the TP (Liu et al. 2013; Li et al. 2015; Liu et al. 2015). In addition, the majority of dust at the surface and lower troposphere of the TP is subsidized by local dust (Mao et al. 2013). These dust particles are aerosols that are present in the atmosphere and are coupled with clouds and

deposited during precipitation. Previous research using an ice core (Kang et al. 2010b) and wet precipitation in the TP (Li et al. 2015) also used Ca^{2+} as a proxy for dust. The present study used the following equation to calculate the EF value (Khare et al. 2004; Khan et al. 2018):

$$EF_{sea} = \frac{(x/\text{Na}^+)_{rainwater}}{(x/\text{Na}^+)_{seawater}} \quad (4)$$

$$EF_{soil} = \frac{(x/\text{Ca}^{2+})_{rainwater}}{(x/\text{Ca}^{2+})_{soil}} \quad (5)$$

where X denotes the desired ion; $(X/\text{Na}^+)_{rainwater}$ and $(X/\text{Ca}^{2+})_{rainwater}$ specify the ratio of the ion of interest with Na^+ and Ca^{2+} in the precipitation, respectively; and $(X/\text{Na}^+)_{seawater}$ and $(X/\text{Ca}^{2+})_{soil}$ symbolize the ratio of the ion of interest with Na^+ and Ca^{2+} in the precipitation and soil, respectively. The standard value for the ratio of seawater and soil was adapted from Xiao (2016).

For the estimation of ion sources in the precipitation, the contribution of marine, crustal, and anthropogenic fractions (represented as SSF, CF, and AF, respectively) were calculated using the following equation (Liu et al. 2015):

$$SSF(\%) = \frac{(x/\text{Na}^+)_{seawater}}{(x/\text{Na}^+)_{rainwater}} \times 100 \quad (6)$$

$$CF(\%) = \frac{(x/\text{Ca}^{2+})_{soil}}{(x/\text{Ca}^{2+})_{rainwater}} \times 100 \quad (7)$$

$$AF(\%) = 100 - SSF - CF \quad (8)$$

Assessment of long-range transport of moisture sources for ions and isotopes Even though trajectory analysis determines the general, rather than the exact, flow of air mass, it has been used in relevant studies for determining the long-range transport of atmospheric components (Li et al. 2015). The Hybrid Single-Particle Lagrangian Integrated Trajectory Model (HYSPLIT Version 4.9) developed by the NOAA Air Resources Laboratory with 7-day backward trajectories was computed to determine the complex pathways of the air masses entering the sampling site (90.36° E, 28.90° N, 1000 m above surface level) (<http://www.arl.noaa.gov/ready/hysplit4.html>). National Center for Environmental Prediction Final Analysis (NCEP FNL) Operational Model Global Tropospheric Analysis datasets with a time interval of six hours and spatial precision of 1.0° from longitude-latitude grids at 500 hPa were used to determine the atmospheric circulation (<https://rda.ucar.edu/datasets/ds083.2/index.html>). This was computed by NCL (NCAR Command Language) software version 6.4.0.

2.4.4 Wet deposition flux and variability

Wet deposition fluxes of the major ions in the precipitation were calculated with the following equation (Zhang et al. 2012):

$$Q_i = 0.01 \times C_i \times P_i \quad (9)$$

where Q_i (eq hm^{-2}) is the ionic flux in the precipitation event, C_i ($\mu\text{eq L}^{-1}$) signifies the ionic concentration in each sample, P_i (mm) indicates the precipitation amount corresponding to the event sample, and 0.01 represents the shift coefficient for the unit.

3 Results and discussion

3.1 Variability in pH and EC

Natural rainwater is weakly acidic, i.e., pH 5.61 (Charlson and Rodhe 1982) due to the reaction of atmospheric CO_2 with rainwater, forming carbonic acid. In this study, the pH of the precipitation ranged from 6.18 to 8.14 with a mean of 6.83 ± 0.45 , which was higher than the natural value, indicating that the alkaline nature of the dust particles is a major determinant of basic pH in the TP (Zhang et al. 2002). The pH of 82% of the samples ranged from 6 to 7, whereas that of the remaining 18% of samples ranged from 7 to 8.13. The effect of low partial CO_2 pressure on pH in the TP is negligible, and the neutralization of carbonate in the tropospheric layer could be the major reason for the alkaline pH (Liu et al. 2013). Similarly, studies conducted in Nam Co (Li et al. 2007) and Lijiang (Zhang et al. 2014) also reported an alkaline pH.

The range in electrical conductivity (EC) in the rainwater was 2.50 to $59.0 \mu\text{S cm}^{-1}$ with a mean value of $15.36 \pm 11.67 \mu\text{S cm}^{-1}$, indicating negligible mineralization. The pH and EC values were observed to be higher in 2017 (i.e., pH - 6.86 ± 0.52 , EC - $21.15 \pm 16.62 \mu\text{S cm}^{-1}$) than in 2016 (pH - 6.81 ± 0.41 , EC - $12.22 \pm 6.09 \mu\text{S cm}^{-1}$). The higher electrical conductivity suggested a higher ionic concentration in the year 2017 (sum of measured ions = $305.3 \mu\text{eq L}^{-1}$) than in 2016 (sum of measured ions = $201 \mu\text{eq L}^{-1}$), symbolizing the direct influence of measured ions on EC during the study period (Fig. 2).

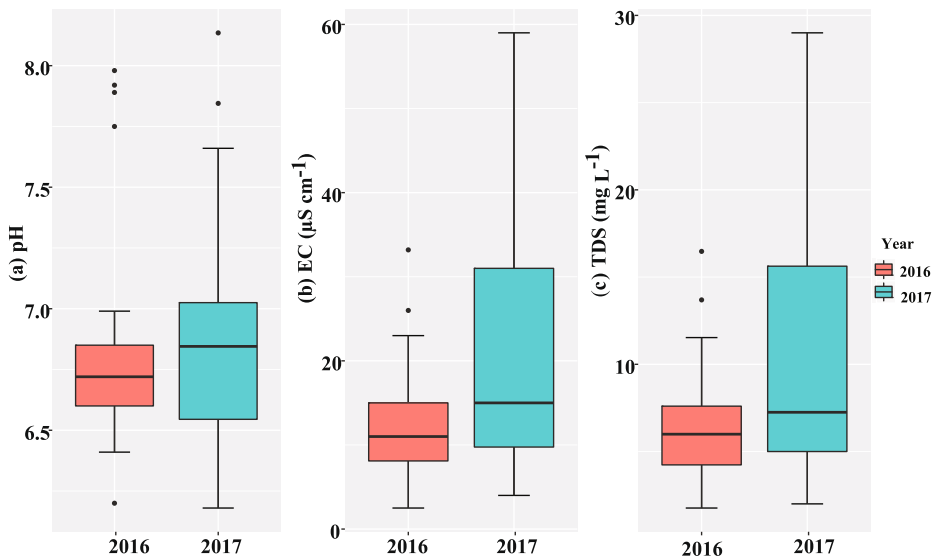


Fig. 2 pH, EC and TDS of precipitation at Wengguo, the northern slopes of Himalayas. The central rectangle extends the first quartile to the third quartile. A segment inside the rectangle expresses the median and, “whiskers” above and below the box demonstrate the positions of the minimum and maximum whereas dots represent outliers

3.2 Characterization of major ionic species

The fraction of both acidic and alkaline components characterize the chemical composition of precipitation. The VWM concentrations of the major ions in comparison with the adjoining sites are presented in Table 1. The sum of the VWM of the major ions was $218.53 \pm 22.08 \mu\text{eq L}^{-1}$, which is higher than Lijiang, Southeast TP ($130.95 \mu\text{eq L}^{-1}$) (Zhang et al. 2014). The VWM percentage of the individual ion to the total ionic mass in the precipitation is presented in Fig. S4. Overall, the ionic abundance follows the pattern of $\text{Ca}^{2+} > \text{HCO}_3^- > \text{Na}^+ > \text{SO}_4^{2-} > \text{Cl}^- > \text{NO}_3^- > \text{K}^+ > \text{Mg}^{2+}$. Of these ions, Ca^{2+} contributes 27.5% of the total mass of the ions, whereas HCO_3^- contributes 22.27% of the total mass of the ions. The higher VWM concentration of Ca^{2+} and HCO_3^- represents the influence of typical crustal dust abundance in calcium (Zhang et al. 2012). Among the anions, SO_4^{2-} was the second abundant one. The concentrations of SO_4^{2-} and NO_3^- in study sites usually specify the impact of anthropogenic activities.

3.3 Neutralizing factor

H_2SO_4 , HNO_3 , and organic acids are principal contributors for the acidity of precipitation (Kaya and Tuncel 1997). The VWM concentrations of SO_4^{2-} and NO_3^- were $38.37 \mu\text{eq L}^{-1}$ and $6.78 \mu\text{eq L}^{-1}$, respectively, which is nearly four and three times greater than the proposed background hemisphere values (Pio et al. 1991), but lower than the densely populated and highly polluted Indo-Gangetic Plain in India (Tiwari et al. 2016). It is suggested that 82.45% of rainwater acidity can be attributed to SO_4^{2-} and 17.54% to NO_3^- , which was calculated from the ratio of $\text{NO}_3^- / (\text{SO}_4^{2-} + \text{NO}_3^-)$. The average ratio of $(\text{NO}_3^- + \text{Cl}^-) / \text{SO}_4^{2-}$ was 0.72, which was lower than the unit reflecting the major impact of sulfuric acid in precipitation (Khemani et al. 1994). The value was lower than that observed in the Northwestern Himalayan region in India (Tiwari et al. 2012). The mean of the ratio between $\text{SO}_4^{2-} / \text{NO}_3^-$ in this study was 8.23. This value was lower than those observed in Guaiba, Brazil (Migliavacca et al. 2005) and Puding, Southwest China (Wu et al. 2012), but higher than the value in the monsoon season observed in Lijiang, Southeast TP (Zhang et al. 2014).

The neutralization of precipitation due to alkaline components is mostly derived from natural sources and biomass burning, which was assessed based on the crustal component and K^+ , respectively. The NF values for Ca^{2+} , K^+ , and Mg^{2+} were 1.07, 0.12, and 0.06, respectively, displaying the abundance of NO_3^- and SO_4^{2-} , which might be a key buffering agent for controlling the acidity stimulated by SO_4^{2-} and NO_3^- . During the study period, it is clear that Ca^{2+} is the dominant neutralizing agent, while minimal neutralization is contributed by K^+ and Mg^{2+} , which is similar to the result from developing urban sites in southeast China (Zhang et al. 2007) and Southeast Tibet (SET) (Zhang et al. 2012).

3.4 Source apportionment of the major ions

3.4.1 Principal component and correlation analysis

The PCA grouped the dataset into two components (Table 2). The first and second component explained 44.44% and 32.77% of the total variance, respectively, with a cumulative value of 77.21%. PC1 indicated the high loading of Na^+ , Cl^- , and K^+ , representing similar mixed sources, i.e., sea salt and biomass burning (Tripathee et al. 2017). Sea salt mainly originates

Table 1 Major ions of precipitation at the Wengguo station, the northern slopes of Himalayas and its comparison with nearby sites

Sites	Nature	Periods	Ca ²⁺	Mg ²⁺	K ⁺	Na ⁺	Cl ⁻	NO ₃ ⁻	SO ₄ ²⁻	HCO ₃ ⁻
Wengguo ^{a**}	Remote	2016–2017	60.1 ± 50.3	3.7 ± 4.4	5.5 ± 6.4	40.1 ± 52.8	15.3 ± 18.7	6.8 ± 5.6	38.4 ± 43.4	48.7 ± 44.1
SET station ^{b**}	Remote	2009–2010	34.0	1.7	1.9	6.7	6.7	2.3	2.6	
Nam Co ^{c**}	Remote	2011–2012	7.9	0.9	0.4	1.9	1.1	4.5	2.9	
Qomolangma ^{c**}	Remote	2011–2012	53.4	1.7	4.5	26.0	27.1	0.8	3.2	
Lhasa ^{d*}	Remote city	1998–2000	197.4	10.9	5.1	11.2	9.7	6.9	5.2	231.7
Lijiang ^{e**}	Urban	2009	52.0	8.7	3.4	4.9	5.9	9.3	31.7	
Xian ^{f**}	Urban	2011–2012	478.4	57.9	65.0	109.3	129.9	122.9	446.6	
Gosainkundais ^{g*}	Remote	2011–2012	9.5	2.5	3.9	10.8	15.0	4.4	6.9	21.4
Kathmandu ^{g*}	Urban	2011–2012	39.2	4.6	2.5	3.8	5.2	12.8	16.3	63.4
Singhagadh ^{h*}	Hilly	2005	43.0	20.0	3.0	62.0	64.0	8.0	31.0	52.0
Kothij ^{i**}	Hilly	2006–2007	30.0	10.0	5.0	23.0	28.0	17.0	26.0	6.0
Delhij ^{j**}	Urban	2009–2011	107.7	47.7	3.0	14.4	22.8	29.8	64.9	27.4

**Volume weight mean, *Mean, SET: Southeast Tibet, ^aThis study, ^bZhang et al. 2013; ^cLiu et al. 2015, ^dZhang et al. 2003;

^eZhang et al. 2014; ^fXiao 2016; ^gTripathee et al. 2014, ^hBudhavant et al. 2009, ⁱTiwari et al. 2012; ^jTiwari et al. 2016;

^{a–f}China, ^gNepal, ^{h,j}India. Unit in $\mu\text{eq L}^{-1}$

Table 2 Rotated component matrix for major ions in precipitation from the Wengguo station. The bold letter indicates for PCA loadings regarded as significant. PC1: principal component 1 and PC2: principal component 2 together explain 77.21% of the data's variability

Component ($N=57$)		
Variables	PC1	PC2
Ca ²⁺	0.14	0.94
Mg ²⁺	0.59	0.62
K ⁺	0.74	0.10
Na ⁺	0.93	-0.09
Cl ⁻	0.90	0.25
NO ₃ ⁻	0.38	0.62
SO ₄ ²⁻	0.93	-0.05
HCO ₃ ⁻	0.11	0.91
EC	0.83	0.45
pH	-0.30	0.69
Variance (%)	44.44	32.77

Cumulative of PC1 and PC2 is 77.21%

The data in bold indicates strong loadings

from the Bay of Bengal and the Arabian Sea. K⁺ might be transported from biomass burning in lowlands via moisture. The massive open biomass burning practices in northern India and Nepal (Ram and Sarin 2010) could be one of the possible sources of K⁺ in the plains. Nevertheless, the soil or the sea might not be the source of SO₄²⁻, but it appeared in the first component and might be brought into the region by marine wind, as illustrated by the trajectory analysis. Similar long-range transport of SO₄²⁻ was observed in a high altitude location in India (Budhavant et al. 2009). Ca²⁺, HCO₃⁻, Mg²⁺, and NO₃⁻ contributed to the loadings in PC2, which clearly suggests that the common source of crustal aerosols (Ca²⁺, HCO₃⁻ and Mg²⁺) results from the calcareous nature of the dust and local biogenic sources (NO₃⁻) emitted from regional activities; for instance, dung combustion for heating and cooking (Li et al. 2007). The majority of dust particles at the surface and lower troposphere of the TP is associated with local dust linked with the regional lithology (Mao et al. 2013). Furthermore, the association of Mg²⁺ in PC1 and PC2 clarifies its mixed marine and dust sources.

A correlation matrix is a commonly used statistical tool that determines the affiliation between two variables and elucidates the degree of dependency of one variable to another. A heatmap matrix showing the Pearson's correlation values of the major ionic sources in the precipitation is presented in Fig. 3. EC, i.e., the total dissolved salt, showed a significant positive correlation ($p=0.01$) with all the ions and remarkably higher r values for salts. pH was correlated with Ca²⁺ and HCO₃⁻ ($r=0.56$ and 0.61 , $p=0.01$ respectively), demonstrating the control of pH by crustal dust, which prevents the region from acidic precipitation. The correlation observed between Ca²⁺, HCO₃⁻, Mg²⁺, and NO₃⁻ ($r=0.55$ to 0.85 , $p=0.01$) suggests the association of crustal dust with anthropogenic components, which is a common occurrence that might be elucidated by the combined impact of crust material together with the absorption of acid species in tropospheric regions (Calvo et al. 2010). The correlation of K⁺, Na⁺, Cl⁻, and SO₄²⁻ ($r=0.54$ to 0.93 , $p=0.01$) suggested the combined sources of biomass burning (natural forest fires and anthropogenic residential), sea salts, and other anthropogenic influences. Moreover, the correlation of Mg²⁺ with sea salt ions demonstrated that it is influenced by marine sources (Zhang et al. 2007). These statistical results of Mg²⁺ explained

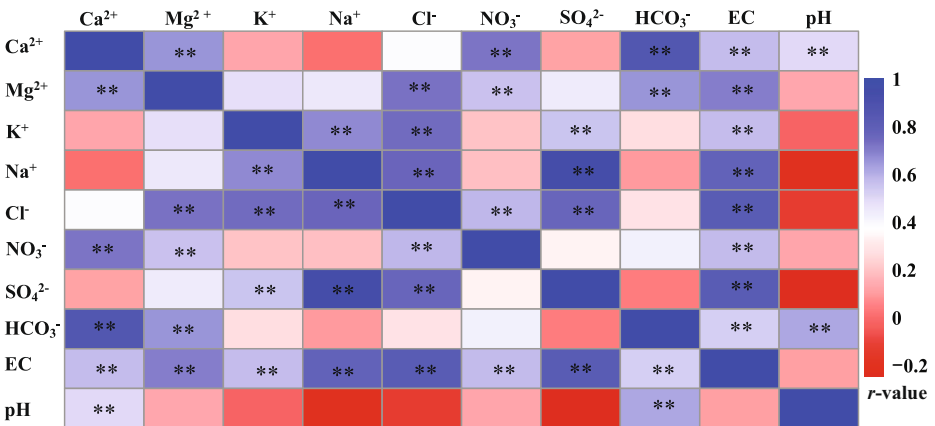


Fig. 3 Heat-map matrix showing Pearson correlation of major ions, pH and EC in precipitation of the Wengguo Station. Symbols (***) inside the cells indicate significance of correlation i.e. $P = 0.01$ level (2-tailed). The scale and color code represent for r value

the combined contributions of crust mineral dust and sea salts. Based on the aforementioned speculation, the source contributions can be categorized into three distinct types, namely crustal mineral dust, sea/marine salts, and anthropogenic sources.

3.4.2 Enrichment factor (EF) and source contribution

The major ions in precipitation originate from the sea, terrestrial environment, and anthropogenic sources. The ratio of the major ions to Na^+ and Ca^{2+} along with the EF values are listed in Table 3. All of the ratios apart from Cl^- were found to be higher than those specified for the seawater ratios, demonstrating the contribution of anthropogenic and crustal sources (Kulshrestha et al. 2003). The EF_{sea} of Cl^- was close to 1, signifying the marine salt origin, which might be attributable to long-range transport from the sea. NO_3^- and SO_4^{2-} were mostly from anthropogenic sources, as their enriched values suggested that they were not derived from sea salt or crustal sources, whereas Ca^{2+} , HCO_3^- , and Mg^{2+} represented cluster carbonate sources. However, the EF_{sea} of Mg^{2+} near 1 represented a sea source.

The source contribution of the major ions in the precipitation is presented in Fig. 4a. It was concluded that almost all the Na^+ and Cl^- in the precipitation samples in the Wengguo station originated from a marine source ($\text{SSF} > 99\%$). Furthermore, Ca^{2+} and HCO_3^- mainly appeared from crustal sources ($\text{CF} = 99.2\%$ and 99.86% , respectively), while NO_3^- and SO_4^{2-} composition was influenced by anthropogenic activities ($\text{AF} = 91.63\%$ and 98.58% , respectively). It

Table 3 Enrichment factors (EFs) relative to seawater (EF_{sea}) and soil (EF_{soil}) for precipitation components

	$\text{HCO}_3^-/\text{Na}^+$	Cl^-/Na^+	K^+/Na^+	$\text{Mg}^{2+}/\text{Na}^+$	$\text{Ca}^{2+}/\text{Na}^+$	$\text{SO}_4^{2-}/\text{Na}^+$	$\text{NO}_3^-/\text{Na}^+$
Seawater	0.0049	1.16	0.02	0.23	0.04	0.12	0.00002
Precipitation	3.48	1.05	0.29	0.26	5.48	1.77	0.63
EF_{sea}	710.20	0.91	13.02	1.14	124.48	14.62	31,500.0
	$\text{NO}_3^-/\text{Ca}^{2+}$	$\text{Cl}^-/\text{Ca}^{2+}$	$\text{K}^+/\text{Ca}^{2+}$	$\text{Mg}^{2+}/\text{Ca}^{2+}$	$\text{SO}_4^{2-}/\text{Ca}^{2+}$	$\text{Na}^+/\text{Ca}^{2+}$	
Soil	0.0021	0.0031	0.50	0.56	0.019	0.57	
Precipitation	0.15	0.40	0.17	0.07	1.23	1.27	
EF_{soil}	70.89	130.26	0.33	0.12	65.54	2.24	

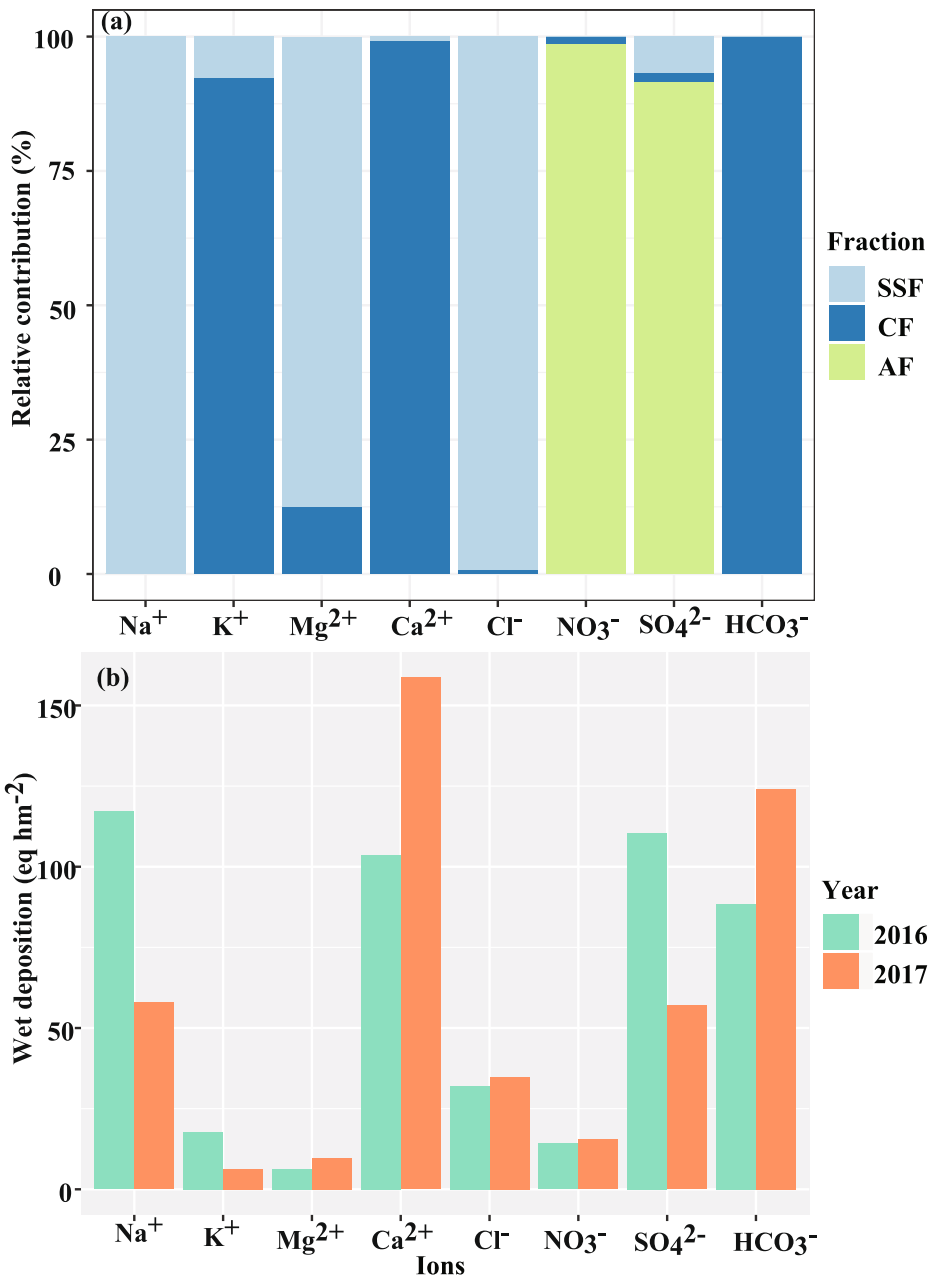


Fig. 4 (a) Source contribution (%) for major ions in precipitation. SSF: sea salt fraction; CF: crust fraction; AF: anthropogenic fraction (b) Water-soluble ionic deposition (eq hm⁻²) in precipitation during summer monsoon of 2016–2017 over the Wengguo Station

was determined that 87.43% of Mg²⁺ appeared to be of marine origin. Previous studies show that K⁺ can be sourced from soil, dust, and biomass burning (Khare et al. 2004; Zhang et al. 2007). In this study, the source contribution calculation of K⁺ showing a crustal source was not

consistent with the results of the correlation analysis (non-significant correlation between Ca^{2+} and K^+) and EF (low EF_{soil} value). Considering the uncertainty in the $\text{K}^+/\text{Ca}^{2+}$ ratio of the background soil used in eq. (7), the major source of K^+ is more likely to be dominated by biomass combustion.

3.5 Wet deposition flux and variability

An average deposition flux of $\text{Ca}^{2+} > \text{HCO}_3^- > \text{Na}^+ > \text{SO}_4^{2-} > \text{Cl}^- > \text{NO}_3^- > \text{K}^+ > \text{Mg}^{2+}$ was calculated during the monsoon period (2016 and 2017). The variability in the wet deposition fluxes for ionic species is presented in Fig. 4b and the variation from year to year in the same season was due to the differences in precipitation quantity and concentration. In our study, the wet deposition of the acidic ionic component (SO_4^{2-}) was higher when the precipitation quantity increased. Conversely, the deposition for alkaline species diminished with increased precipitation quantity. The deposition of ionic species (Na^+) associated with long-range transport was higher with increased precipitation quantity. Similar results were observed in research conducted in the Indian Plain (Tiwari et al. 2016). However, the deposition of ionic constituents related to local biogenic sources (NO_3^-) hardly differed in the two years. The deposition of Cl^- in 2016 was slightly lower than in 2017, which might be due to the loss of Cl^- in the atmosphere by complex chemical processes (Wu et al. 2006). It was interesting that K^+ flux was decreased in 2017, suggesting less deposition during this year, which could be related to low biomass burning or forest fire as compared to 2016 and was confirmed by the fire spot observed by MODIS (Fig. S5). The annual monsoon fluxes of the total measured ions were 490.0 and 463.89 eq hm^{-2} for 2016 and 2017, with a corresponding annual rainfall of 264.6 and 171.9 mm, respectively. This represents approximately 3% higher deposition under 21.23% higher rainfall during 2016 as compared to 2017, signifying the influence of precipitation quantity.

The wet deposition fluxes were compared with an inland (Nam Co, Lhasa, Waliguan) and coastal site (Tokoro), as well as previous data obtained from Zhang et al. (2012). The fluxes of Ca^{2+} (131.15 ± 38.85 eq hm^{-2}) and HCO_3^- (106.22 ± 25.27 eq hm^{-2}) at Wengguo were higher than at the Nam Co station ($\text{Ca}^{2+} - 86.26$ eq hm^{-2} and $\text{HCO}_3^- - 98.66$ eq hm^{-2}) but lower than Lhasa ($\text{Ca}^{2+} - 987.0$ eq hm^{-2} and $\text{HCO}_3^- - 1158.50$ eq hm^{-2}). The SO_4^{2-} (83.74 ± 37.78 eq hm^{-2}) deposition was much higher than Nam Co (33.32 eq hm^{-2}) and Lhasa (26.0 eq hm^{-2}) but lower than Waliguan (93.12 eq hm^{-2}). Moreover, the flux of Na^+ (87.50 ± 41.87 eq hm^{-2}) and Cl^- (33.42 ± 1.97 eq hm^{-2}), which was strongly influenced by the long-range transport from marine source, was much higher than Nam Co ($\text{Na}^+ - 34.50$ eq hm^{-2} and $\text{Cl}^- - 27.62$ eq hm^{-2}) and Waliguan ($\text{Na}^+ - 33.76$ eq hm^{-2} and $\text{Cl}^- - 23.67$ eq hm^{-2}) but lower than Tokoro, Japan ($\text{Na}^+ - 2916.8$ eq hm^{-2} and $\text{Cl}^- - 3297.87$ eq hm^{-2}). As a result, wet deposition fluxes of the major ions at the pristine Wengguo station suggested that major ionic deposition not only originates from natural crustal dust but also from the long-range transport of marine salt sources from the Indian Ocean and moisture associated with anthropogenic ions from South Asia.

3.6 Characteristics of the stable isotopes

Moisture source, precipitation mechanism, and rainfall duration impact the distribution of stable isotopes in precipitation (Yu et al. 2007a). The $\delta^{18}\text{O}$ value ranged from -29.16 ‰ to -3.30 ‰, with a mean value of -15.22 ± 5.17 ‰, whereas δD ranged from -224.13 ‰ to

−19.13 ‰, with a mean value of -116.01 ± 41.31 ‰. The abrupt changes in stable isotopes with precipitation quantity (Fig. 5) illustrated the low value of isotopes with intense precipitation and vice versa. Previous research conducted in Lhasa (Yu et al. 2008) reported similar mean values (1991 to 1999: -17.38 ‰ and 2000–2003: -16.06 ‰) for the oxygen isotopes in precipitation. Similarly, a study in Bomi (Gao et al. 2015) reported similar ranges of $\delta^{18}\text{O}$ (monsoon: -0.5 ‰ to -29.1 ‰) influenced by monsoonal activities for the lower value of isotopes corresponding to higher precipitation amounts. Generally, the isotopic composition during the study period was depleted in July of the other years, but the value was higher in July 2015, which could be associated with the low relative humidity in comparison to the other years, representing a drier condition that results in sub-cloud evaporation. Due to the inaccessibility of data for relative humidity in September 2014, the depletion of stable isotopes could not be confirmed, but it also might be linked with relative humidity and precipitation amount. Out of the four-event samples in the first week of September, two events had low isotopes corresponding to large precipitation amounts (1st Sep - $\delta^{18}\text{O}$: -21.74 ‰, δD : -159.51 , PP: 10.3 mm and 4th Sep - $\delta^{18}\text{O}$: -23.80 ‰, δD : -178.58 , PP: 11.2 mm), resulting in the low isotopes in that month.

The affiliation of rainfall quantity and temperature with isotopic composition was first observed by Dansgaard (1964). The relationship between climate variables and isotopes in long-term rainfall events during the monsoon (2013 to 2017) was also analyzed in this study. The dataset indicated the existence of a negative correlation between stable isotopes and precipitation and a positive correlation between stable isotopes and temperature. The correlation of isotopes with precipitation was significant ($p < 0.01$), whereas the correlation with temperature was not significant ($p > 0.05$) (Fig. S6), suggesting that rainfall quantity has a pivotal role in controlling stable isotopes during summer in the study site.

Stable isotope values were diminished sharply during the monsoon period, which might be associated with the moisture from low-level sea surface evaporation. The Bay of Bengal acts as

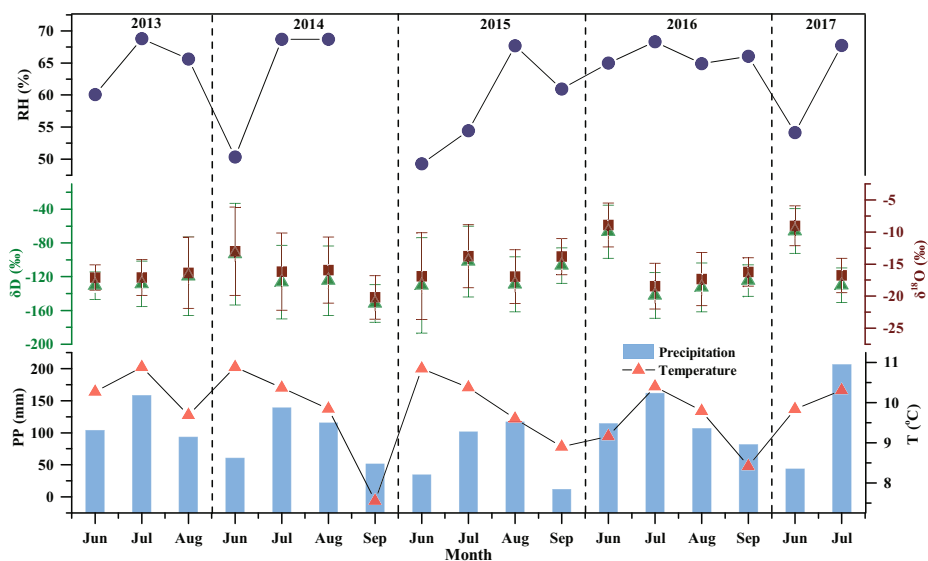


Fig. 5 Temporal variation in precipitation stable isotopes ($\delta^{18}\text{O}$ and δD) at the Wengguo Station, and temperature (T), precipitation (PP) and relative humidity (RH) at the nearby Langkazi station during monsoon period of 2013–2017

a key source of moisture for the abrupt decline of isotopes during precipitation in the early monsoon period (Yang et al. 2012), followed by the Indian monsoon from the south Indian Ocean, which might be another major moisture source accounting for the dramatic decrease in precipitation isotopes of the active monsoon period (Yao et al. 2013). Moreover, the rainout mechanism during the long-range transport of moisture from low to high-level results in a stable isotopic fractionation that subsidizes low, stable isotopes in precipitation (Tian et al. 2001b). Continuous substantial precipitation led to gradual negative isotopic values in Wengguo, which is also explained by the negative correlation between stable isotopes with rainfall amount at this site (Zhao et al. 2018). Local surface air temperature, precipitation amount, and relative humidity are classical ways of understanding the variations in stable isotopes in precipitation. The observed isotopic variability during the five-year wet period might be associated with variation in local climatic variables and the large-scale mode of atmospheric circulation (Gao et al. 2017).

3.7 Deuterium excess and meteoric water line

The transformation of water to different phases alters the composition of the stable isotopes in the precipitation, which undergo fractionation due to temperature and moisture, resulting in differences in the stable isotopes. Deuterium excess expressed as d , where ($d = \delta D - 8 \delta^{18}O$) (Dansgaard 1964) specifies the non-equilibrium (deuterium excess is 0 ‰ when condensation occurs in equilibrium condition) isotopic effect is one of the useful tracers of the global hydrological cycle because its value relies on the difference in fractionation velocity of 2H and ^{18}O (Qu et al. 2018). Moreover, it represents the rate of evaporation in the region, which is dependent on relative humidity (Chhetri et al. 2014). The global mean value of d -excess is 10 ‰ under the global average condition that characterizes the meteorological circumstance of the source region (Pfahl and Sodemann 2014). The kinetic fractionation will be strengthened in the course of evaporation under dry climate conditions, and the d -excess value in the subsequent precipitation will be higher than the global mean value (> 10 ‰). However, during humid climate conditions, the kinetic fractionation in the evaporation will be weakened, resulting in a low d -excess value (< 10 ‰) (Yu et al. 2007b).

The relative humidity at Wengguo during the study period ranged from 62% to 66%, with a mean value of $63 \pm 3.07\%$. The variation in the d value in precipitation at Wengguo station fluctuated significantly (-14.62 to 19.35 ‰, mean: 5.81 ± 5.43 ‰) and was lower than 10 ‰ (global mean), thus indicating the partial evaporation of raindrops. Out of 178 samples, the d -excess value of 81.46% of the samples was lower than the global mean value. The monthly average and annual mean value along with the event data during the monsoon period for the year 2013 to 2017 were also reported (Fig. 6). The total average and each annual mean value obtained in this study are higher than in Kathmandu (4.02 ‰) in the southern slopes of the Himalayas but lower than Mawlong (11.89 ‰), which is closer to the Bay of Bengal (Chhetri et al. 2014). The lower d -excess during the monsoon suggests high relative humidity over the primary source region, i.e., the moisture from a humid oceanic source such as the Indian Ocean and/or Bay of Bengal (Chakraborty et al. 2016; Yu et al. 2016). The values in August (2013) and June (2014) were slightly higher than the global mean, which was probably triggered by re-evaporation (Qu et al. 2018). Hence, the substantial alteration in stable isotopes and d -excess values directs the occurrence of monsoon moisture transport systems from the lowlands to highlands. Based on trend analysis using Kendall's tau-b test, the five-year annual mean d -

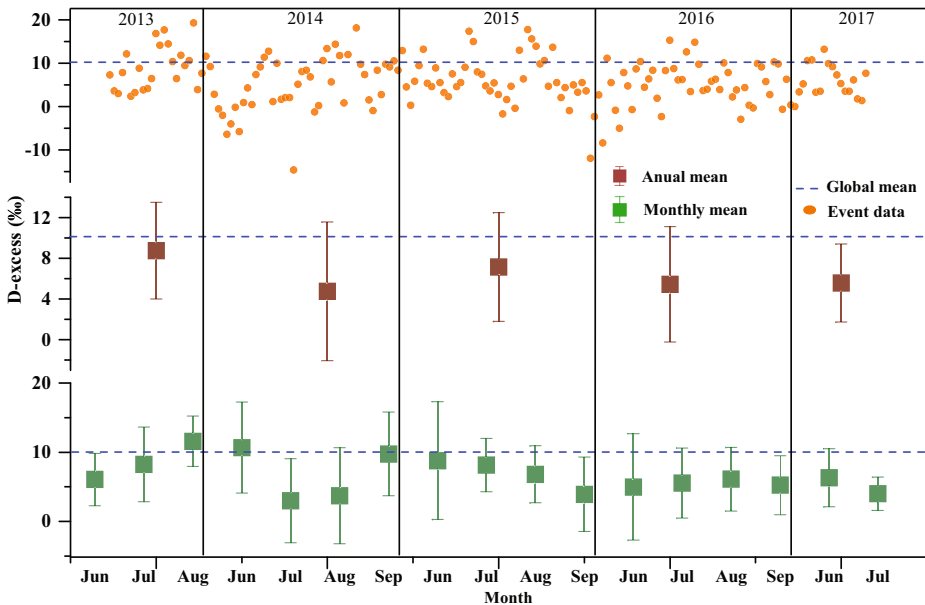


Fig. 6 D-excess value for the Wengguo Station, Southern Tibetan Plateau. The dashed line characterizes the global mean value ($\sim 10\text{‰}$)

excess revealed a decreasing trend but not significant. The variability of d-excess could be concomitant with both variation in local climatic variables and the large-scale atmospheric circulation (Gao et al. 2017).

The global meteoric water line (GMWL) $\delta D = (8.20 \pm 0.07) \delta^{18}\text{O} + (11.27 \pm 0.65)$ represents the average global freshwater composition (hydrogen and oxygen isotopes) (Rozanski et al. 1993). The lower value of the slope and intercept determined by the linear regression line between $\delta^{18}\text{O}$ and δD indicates that the raindrops are subjected to extreme evaporation (Qu et al. 2018). In this study, the slope and intercept of the local meteoric water line ($\delta D = 7.91\delta^{18}\text{O} + 4.48$), abbreviated as LMWL, differed from GMWL, demonstrating the limited effect of non-equilibrium processes on precipitation (Fig. 7). This value is very near to the slope of LMWL obtained at Lasha (7.9) (Tian et al. 2001a) and Bomi (7.85) in the southern TP (Gao et al. 2015). Owing to the limited difference between LMWL with GMWL, ocean air constitutes the chief source of moisture for the study site in the monsoon season (Zhao et al. 2018).

3.8 Air mass backward trajectory analysis and water vapor flux

Figure 8 displays the 7-day backward trajectories of the air mass approaching the sampling site. The cluster trajectories indicated that a large number of air masses at Wengguo station were transported from South Asia during the study period. The majority of the air masses that reached the sampling site were from Bangladesh, northeast India, western Myanmar, and Bhutan, indicating that the moisture originating from the Bay of Bengal was transported with an abundance of polluted air from the urban cities and Indo-Gangetic Plain. Moreover, the Bay of Bengal is the source zone of monsoon precipitation, which is supported by monthly water vapor at 500 hPa (Fig. 9) resulting in lower isotope values in the monsoon domain, Wengguo. Thus, according to the cluster analysis of the backward trajectories and NCEP FNL dataset, the

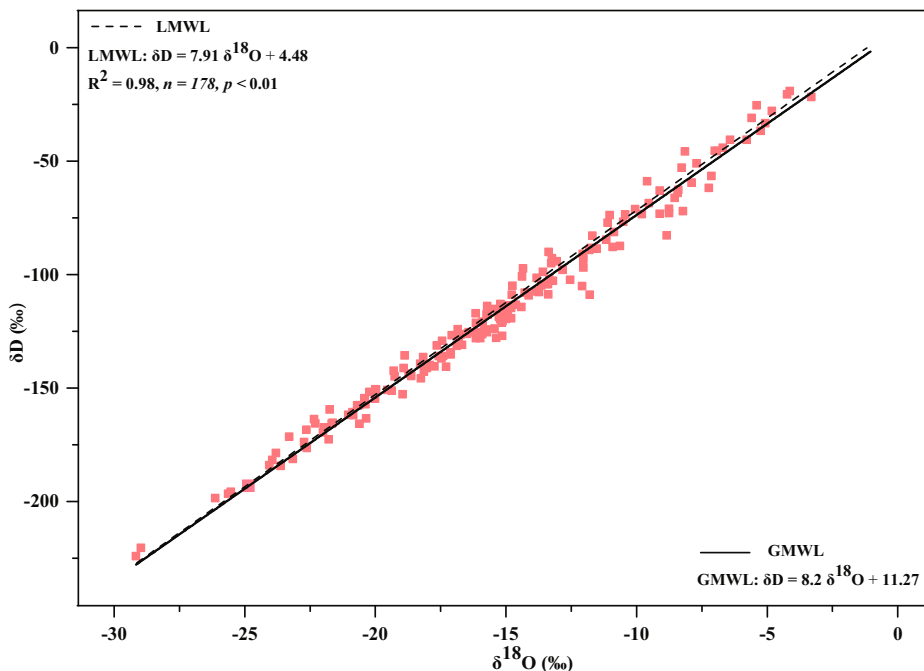


Fig. 7 Comparison of the local meteoric water line (LMWL) for the study area with the global meteoric water line (GMWL)

moisture sources indicated that most of the trajectories arrived from warm and humid low-latitude regions. The moisture source was not only responsible for the precipitation but also transported pollution from the lowlands to the pristine TP. Therefore, wet deposition at Wengguo is predominantly influenced by the anthropogenic emissions in South Asia.

4 Uncertainty and recommendations

A quantitative assessment of wet deposition fluxes of major ions and isotopic characteristics during the monsoon season in the Wengguo hydrological station of the southern TP was conducted to identify the basic characteristics of the ions and isotopes in the precipitation and the potential sources. This study provides information regarding the influence of monsoon moisture sources for the transportation of ions from lowlands to pristine southern TP as evidenced by the isotopic characteristics. However, some uncertainties in this evaluation still exist. A more accurate description of deposition and multiple sources will be identified through long-term annual monitoring, as the TP is influenced by both monsoon and westerlies, whereas we only estimated the deposition in the monsoon season. Similar to Ca^{2+} , NH_4^+ is another neutralizing component in the atmosphere that was not evaluated in this study due to some technical issues. HCO_3^- was calculated based on the ion balance method, which considers the deficiency of the anions and the characteristics of the surrounding environment (alkalinity of soil and rainwater). Nonetheless, NH_4^+ was minimal in the environment. It is not important to estimate the bicarbonate in the ion balance method, and our result was supported by the regression of the sum of the ions and TDS after calculating bicarbonate, which indicated good data quality.

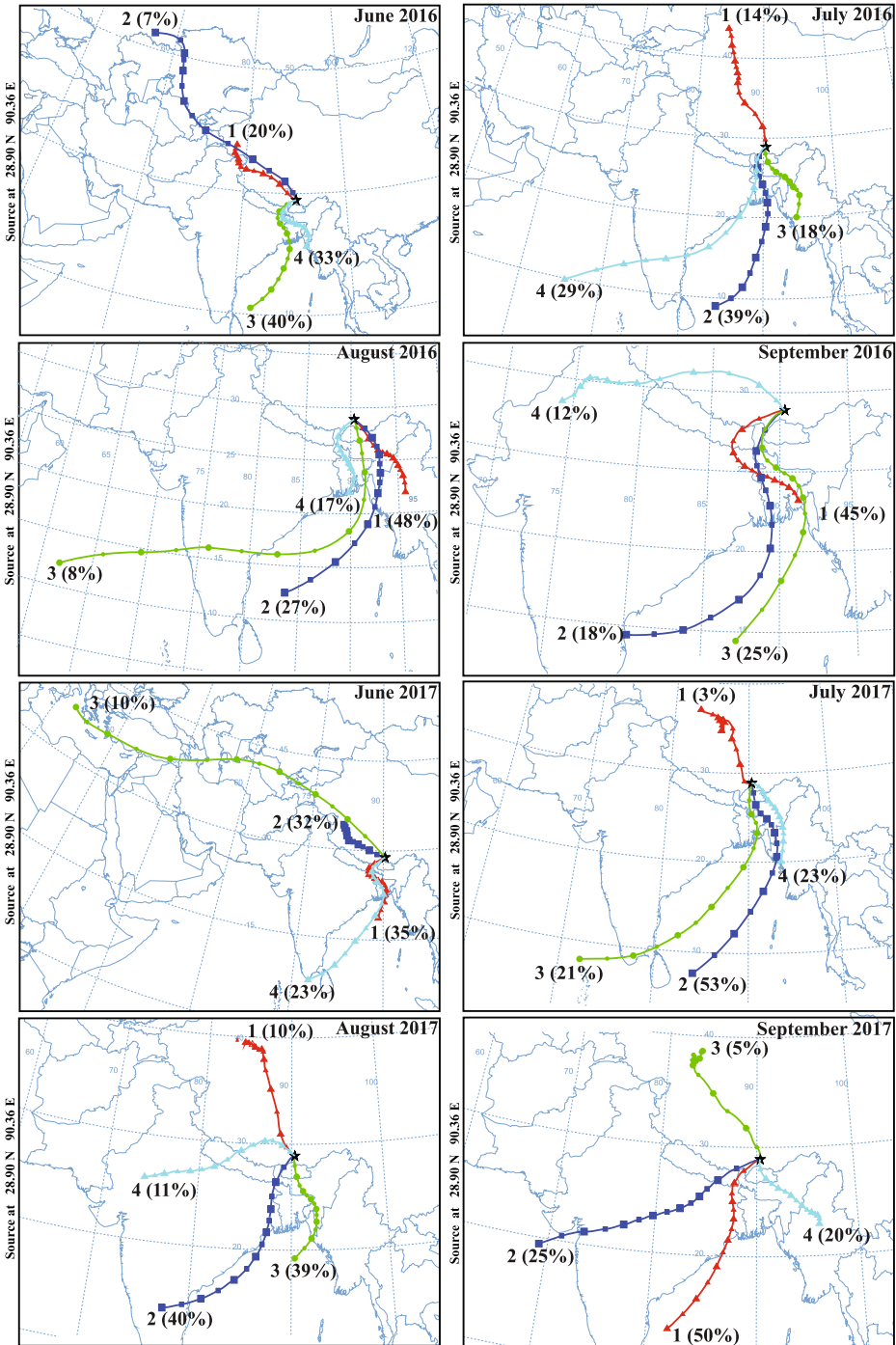


Fig. 8 Clusters of seven-day air mass backward trajectories at the Wengguo Station in the Southern TP

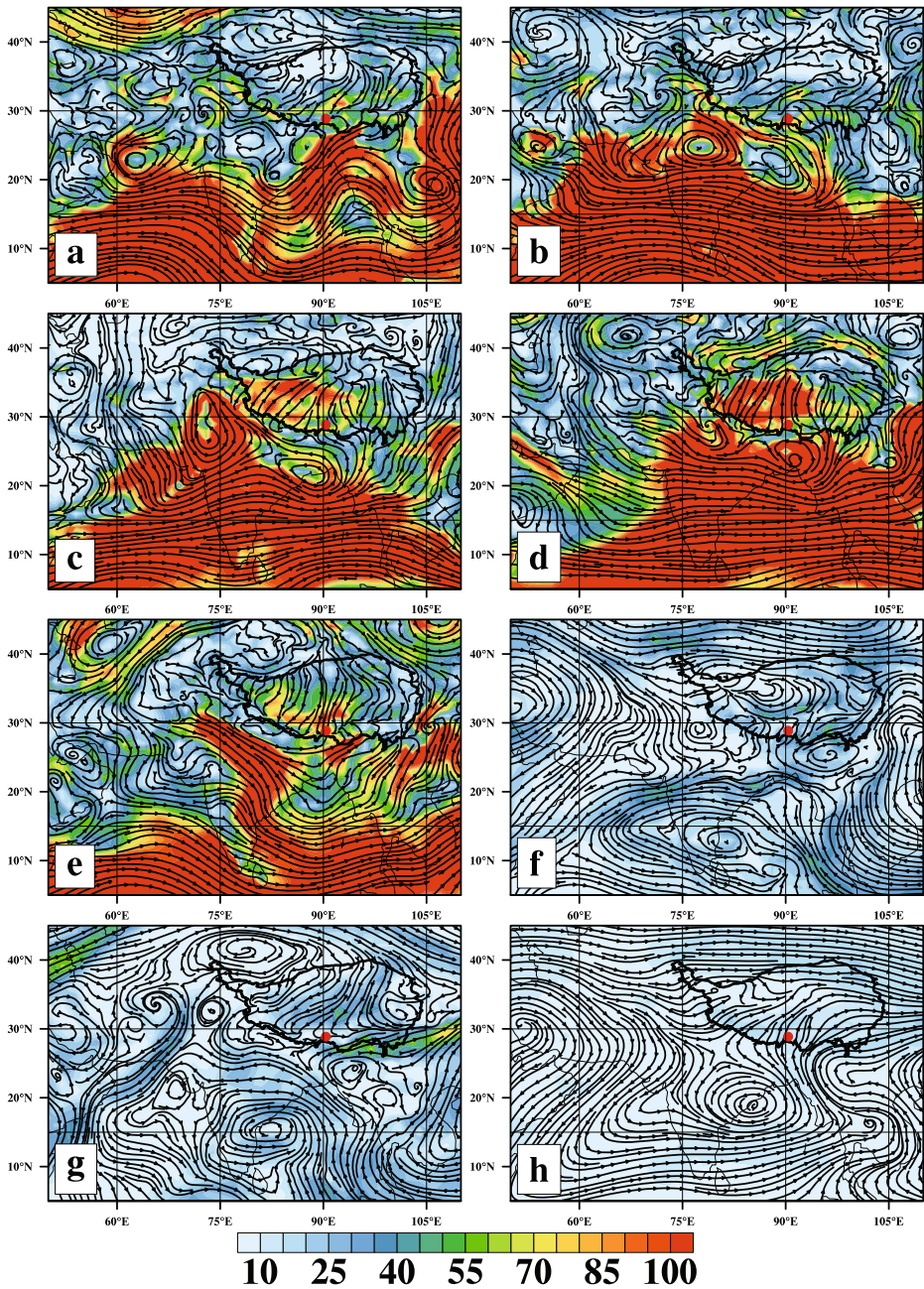


Fig. 9 Circulation of the wind fields calculated by the NCEP FNL Operational Model Global Tropospheric Analysis datasets, with a time interval of six hours and a spatial precision of 1° from longitude-latitude grids at 500 hPa during monsoon season over the Wengguo station, Tibetan Plateau (denoted by solid red dot), a: Aug 7 (2013), b and c: July 24 and Sep 04 (2014), d and e: Jun: 25 and July 14 (2015), f: July 21 (2016), g: July 08 (2017), h: Average JJAS (2013–2017). The scale bar represents the vapor flux in 10^{-1} g/cm.hpa

5 Conclusion

The continuous monitoring of monsoon precipitation for ions and isotopes was investigated to determine the physicochemical driving factors at the Wengguo hydrological station in the southern TP. The collective chemical, isotopic, and air mass analyses elucidated the sources of the major ions in the precipitation in the atmosphere of Wengguo. The average pH and electrical conductivity of the precipitation at Wengguo were 6.82 ± 0.45 and $15.36 \pm 11.67 \mu\text{S cm}^{-1}$, respectively, with a higher electrical conductivity value in 2017, which indicated a higher ionic concentration with lower precipitation in comparison to 2016. During the observation period, the VWM concentration of the ions was in the order $\text{Ca}^{2+} > \text{HCO}_3^- > \text{Na}^+ > \text{SO}_4^{2-} > \text{Cl}^- > \text{NO}_3^- > \text{K}^+ > \text{Mg}^{2+}$, confirming the higher impact of typical crustal dust followed by sea salt and anthropogenic sources. Likewise, the low concentration of K^+ in 2017 was indicative of low biomass burning as compared to 2016. Throughout the study period, the principal neutralizing ionic species were $\text{Ca}^{2+} > \text{K}^+ > \text{Mg}^{2+}$.

The wet deposition fluxes of the total measured ions were 490.0 and 463.89 eq hm^{-2} for 2016 and 2017, respectively, representing 3% higher deposition during 2016 and corresponding to a 21.23% higher precipitation amount. The ratio of $\text{SO}_4^{2-} / \text{NO}_3^-$ reflected the mean value of 7.9. The PCA and correlation analysis suggested three distinct sources of major ions: 1) anthropogenic (SO_4^{2-} , NO_3^-) and biomass burning (K^+), 2) long-distance sea salts (Na^+ , Cl^- and Mg^{2+}), and 3) local crustal dust (Ca^{2+} , HCO_3^- , and Mg^{2+}) over Wengguo. Moreover, the quantity of precipitation has an essential role in governing the stable isotopes during the summer season. Stable isotope values decreased abruptly throughout the monsoon period, which was related to the moisture originating from low-level sea surface evaporation. Based on the variation in the slopes and intercept of LMWL with GMWL, ocean air constitutes the primary moisture source in the study site. Likewise, the extremely low value of the $\delta^{18}\text{O}$ stable isotopes and d-excess values explained the occurrence of continental and monsoon moisture transport systems.

In addition, the moisture sources in the precipitation events were monitored and traced using back-trajectories analyses and the NCEP FNL dataset. The majority of the air masses that reached the sampling site from the Bay of Bengal contained abundant polluted aerosols transported from cities of Bangladesh, northeast India, western Myanmar, Bhutan, and the Indo-Gangetic Plain. This study provides insights into the deposition of major ions and their sources with isotopic fingerprints over Wengguo, TP, which could be a valuable dataset for future studies.

Acknowledgments This research work was financially supported by the National Natural Science Foundation of China (Grant No 41771090) and the Strategic Priority Research Program of the Chinese Academy of Sciences (XDA20060202).

References

- Al-Khashman, O.A.: Study of chemical composition in wet atmospheric precipitation in Eshidiya area Jordan. *Atmos Environ.* **39**(33), 6175–6183 (2005). <https://doi.org/10.1016/j.atmosenv.2005.06.056>
- Budhavant, K.B., Rao, P.S.P., Safai, P.D., Ali, K.: Chemistry of monsoon and post-monsoon rains at a high altitude location, Sinhagad India. *Aerosol Air Quality Res.* **9**(1), 65–79 (2009). <https://doi.org/10.4209/aaqr.2008.07.0033>
- Calvo, A.I., Olmo, F.J., Lyamani, H., Alados-Arboledas, L., Castro, A., Fernández-Raga, M., Fraile, R.: Chemical composition of wet precipitation at the background EMEP station in Viznar (Granada, Spain) (2002–2006). *Atmos. Res.* **96**(2–3), 408–420 (2010). <https://doi.org/10.1016/j.atmosres.2010.01.013>

- Krklec, K., Dominguez-Villar, D.: Quantification of the impact of moisture source regions on the oxygen isotope composition of precipitation over. *Geochim. Cosmochim. Acta.* **134**, 39–54 (2014). <https://doi.org/10.1016/j.gca.2014.03.011>
- Chakraborty, S., Sinha, N., Chattopadhyay, R., Sengupta, S., Mohan, P.M., Datye, A.: Atmospheric controls on the precipitation isotopes over the Andaman Islands Bay of Bengal. *Sci Rep.* **6**, 1–11 (2016). <https://doi.org/10.1038/srep19555>
- Charlson, R.J., Rodhe, H.: Factors controlling the acidity of natural rainwater. *Nature.* **295**(5851), 683–685 (1982). <https://doi.org/10.1038/295683a0>
- Chhetri, T.B., Yao, T., Yu, W., Ding, L., Joswiak, D., Tian, L., Devkota, L.P., Qu, D.: Stable isotopic compositions of precipitation events from Kathmandu, southern slope of the Himalayas. *China Sci Bull.* **59**(34), 4838–4846 (2014). <https://doi.org/10.1007/s11434-014-0547-4>
- Cong, Z., Kang, S., Zhang, Y., Li, X.: Atmospheric wet deposition of trace elements to central Tibetan plateau. *Appl. Geochem.* **25**(9), 1415–1421 (2010). <https://doi.org/10.1016/j.apgeochem.2010.06.011>
- Dansgaard, W.: Stable isotopes in precipitation. *Tellus.* **16**(4), 436–468 (1964). <https://doi.org/10.3402/tellusa.v16i4.8993>
- Deusdará, K.R.L., Forti, M.C., Borma, L.S., Menezes, R.S.C., Lima, J.R.S., Ometto, J.P.H.B.: Rainwater chemistry and bulk atmospheric deposition in a tropical semiarid ecosystem: the Brazilian Caatinga. *J. Atmos. Chem.* **74**(1), 71–85 (2017). <https://doi.org/10.1007/s10874-016-9341-9>
- Gao, J., He, Y., Masson-Delmotte, V., Yao, T.: ENSO effects on annual variations of summer precipitation stable isotopes in Lhasa, southern Tibetan Plateau. *Journal of Climate.* **30**(11), (2017). <https://doi.org/10.1175/JCLI-D-16-0868.1>
- Gao, J., Masson-delmotte, V., Yao, T., Tian, L., Risi, C., Hoffmann, G.: Precipitation water stable isotopes in the south Tibetan plateau : observations and modeling. *J. Clim.* **24**, 3161–3178 (2015). <https://doi.org/10.1175/2010JCLI7376.1>
- Gonfiantini, R.: Standard for stable isotopes. *Nature.* **271** (1978)
- Huang, H., Liu, M., Wang, J., He, J., Chen, H. (2018): Sources Identification of Nitrogen Using Major Ions and Isotopic Tracers in Shenyang , China. *Hindawi Geofluids.* (2018)
- Hughes, C.E., Crawford, J.: Spatial and temporal variation in precipitation isotopes in the Sydney Basin Australia. *J Hydrol.* **489**, 42–55 (2013). <https://doi.org/10.1016/j.jhydrol.2013.02.036>
- Kajino, M., Aikawa, M.: A model validation study of the washout/rainout contribution of sulfate and nitrate in wet deposition compared with precipitation chemistry data in Japan. *Atmos. Environ.* **117**, 124–134 (2015). <https://doi.org/10.1016/j.atmosenv.2015.06.042>
- Kang, S., Xu, Y., You, Q., Flugel, W.A., Pepin, N., Yao, T.: Review of climate and cryospheric change. *Environ. Res. Lett.* **5**, (2010a). <https://doi.org/10.1088/1748-9326/5/1/015101>
- Kang, S., Zhang, Y., Zhang, Y., Grigholm, B., Kaspari, S., Qin, D., Ren, J., Mayewski, P.: Variability of atmospheric dust loading over the central Tibetan plateau based on ice core glaciochemistry. *Atmos. Environ.* **44**(25), 2980–2989 (2010b). <https://doi.org/10.1016/j.atmosenv.2010.05.014>
- Kaya, G., Tuncel, G.: Trace element and major ion composition of wet and dry depositon in Ankara Turkey. *Atmos Environ.* **31**(23), 3985–3998 (1997). [https://doi.org/10.1016/S1352-2310\(97\)00221-5](https://doi.org/10.1016/S1352-2310(97)00221-5)
- Khan, F., Nizam, K., Maulud, A., Talib, M., Xiang, J., Amil, N., Alias, A., Nadzir, M., Sahani, M., Mohammad, M., Jahaya, M., Hassan, H., Jeba, F., Tahir, N., Abdullah, S.: Environment physicochemical factors and their potential sources inferred from long-term rainfall measurements at an urban and a remote rural site in tropical areas. *Sci. Total Environ.* **613–614**, 1401–1416 (2018). <https://doi.org/10.1016/j.scitotenv.2017.08.025>
- Khare, P., Goel, A., Patel, D., Behari, J.: Chemical characterization of rainwater at a developing urban habitat of northern India. *Atmos. Res.* **69**(3–4), 135–145 (2004). <https://doi.org/10.1016/j.atmosres.2003.10.002>
- Khemani, L.T., Momin, G.A., Rao, P.S.P., Pillai, A.G., Safai, P.D., Mohan, K., Rao, M.G.: Atmospheric pollutants and their influence on acidification of rain water at an industrial location on the west coast of India. *Atmos. Environ.* **28**(19), 3145–3154 (1994). [https://doi.org/10.1016/1352-2310\(94\)00148-E](https://doi.org/10.1016/1352-2310(94)00148-E)
- Kolde, R.: Pheatmap. pretty heatmaps. R package version. 1.0.12 (2019)
- Kulshrestha, U.C., Kulshrestha, M.J., Sekar, R., Sastry, G.S.R., Vairamani, M.: Chemical characteristics of rainwater at an urban site of south-Central India. *Atmos. Environ.* **37**(21), 3019–3026 (2003). [https://doi.org/10.1016/S1352-2310\(03\)00266-8](https://doi.org/10.1016/S1352-2310(03)00266-8)
- Kulshrestha, U.C., Sarkar, A.K., Srivastava, S.S., Parashar, D.C.: Wet-only and bulk deposition studies at New Delhi (India). *Water, Air, & Soil Pollution.* **85**(4), 2137–2142 (1995). <https://doi.org/10.1007/BF01186150>
- Li, C., Kang, S., Zhang, Q., Kaspari, S.: Major ionic composition of precipitation in the Nam co region Central Tibetan Plateau. *Atmos Res.* **85**(3–4), 351–360 (2007). <https://doi.org/10.1016/j.atmosres.2007.02.006>
- Li, Z., Li, Z., Wang, T., Gao, Y., Cheng, A., Guo, X., Guo, R., Jia, B., Yaoxuan, S., Han, C., Theakstone, W.H.: Composition of wet deposition in the central Qilian Mountains. *Environment Earth Science.* **73**(11), 7315–7328 (2015). <https://doi.org/10.1007/s12665-014-3907-0>

- Liu, B., Kang, S., Sun, J., Wan, X., Wang, Y., Gao, S., Cong, Z.: Low-molecular-weight organic acids in the Tibetan plateau : results from one-year of precipitation samples at the SET station. *Atmos. Environ.* **86**, 68–73 (2014). <https://doi.org/10.1016/j.atmosenv.2013.12.028>
- Liu, B., Kang, S., Sun, J., Zhang, Y., Xu, R., Wang, Y., Liu, Y., Cong, Z.: Wet precipitation chemistry at a high-altitude site (3,326 m a.s.l.) in the southeastern Tibetan plateau. *Environmental science and Pollut. Res.* **20**(7), 5013–5027 (2013). <https://doi.org/10.1007/s11356-012-1379-x>
- Liu, Y.W., Xu, R., Wang, Y.S., Pan, Y.P., Piao, S.L.: Wet deposition of atmospheric inorganic nitrogen at five remote sites. *Atmos. Chem. Phys.* **15**, 11683–11700 (2015). <https://doi.org/10.5194/acp-15-11683-2015>
- Lu, X., Li, L.Y., Li, N., Yang, G., Luo, D., Chen, J.: Chemical characteristics of spring rainwater of Xi'an city NW China. *Atmos Environ.* **45**(28), 5058–5063 (2011). <https://doi.org/10.1016/j.atmosenv.2011.06.026>
- Mao, R., Gong, D.Y., Shao, Y.P., Wu, G.J., Bao, J.D.: Numerical analysis for contribution of the Tibetan plateau to dust aerosols in the atmosphere over the East Asia. *Sci China Earth Sci.* **56**(2), 301–310 (2013). <https://doi.org/10.1007/s11430-012-4460-x>
- Migliavacca, D., Teixeira, E.C., Wiegand, F., Machado, A.C.M., Sanchez, J.: Atmospheric precipitation and chemical composition of an urban site , Guaiba hydrographic basin Brazil. *Atmos Environ.* **39**, 1829–1844 (2005). <https://doi.org/10.1016/j.atmosenv.2004.12.005>
- Mohan, S.M.: An overview of particulate dry deposition: measuring methods, deposition velocity, and controlling factors. *Int. J. Environ. Sci. Technol.* **13**(1), 387–402 (2016). <https://doi.org/10.1007/s13762-015-0898-7>
- Pfahl, S., Sodemann, H.: What controls deuterium excess in global precipitation ? *Clim. Past.* **10**(1), 771–781 (2014). <https://doi.org/10.5194/cp-10-771-2014>
- Pio, C.A., Salgueiro, M.L., Nunes, T.V.: Seasonal and air-mass trajectory effects on rainwater quality at the south-western european border. *Atmos. Environ.* **25**(10), 2259–2266 (1991). [https://doi.org/10.1016/0960-1686\(91\)90101-C](https://doi.org/10.1016/0960-1686(91)90101-C)
- Pu, W., Quan, W., Ma, Z., Shi, X., Zhao, X., Zhang, L., Wang, Z., Wang, W.: Long-term trend of chemical composition of atmospheric precipitation at a regional background station in northern China. *Sci. Total Environ.* (2016). <https://doi.org/10.1016/j.scitotenv.2016.12.097>
- Qu, S., Chen, X., Wang, Y., Shi, P., Shan, S., Gou, J., Jiang, P.: Isotopic characteristics of precipitation and origin of moisture sources in Hemuqiao catchment, a small watershed in the lower reach of Yangtze River. *Water.* **10**(9), 1170 (2018). <https://doi.org/10.3390/w10091170>
- Pant, R.R., Zhang, F., Rehman, F., Wang, G., Ye, M., Zeng, C., Tang, H.: Spatiotemporal variations of hydrogeochemistry and its controlling factors in the Gandaki River basin, Central Himalaya Nepal. *Sci Total Environ.* **622–623**, 770–782 (2018). <https://doi.org/10.1016/j.scitotenv.2017.12.063>
- Ram, K., Sarin, M.M.: Spatio-temporal variability in atmospheric abundances of EC, OC and WSOC over Northern India. *J Aerosol Sci.* **41**(1), 88–98 (2010). <https://doi.org/10.1016/j.jaerosci.2009.11.004>
- Rao, P.S.P., Tiwari, S., Matwale, J.L., Pervez, S., Tunved, P., Safai, P.D., Srivastava, A.K., Bisht, D.D., Sing, S.N., Hopke, P.K.: Sources of chemical species in rainwater during monsoon and non-monsoonal periods over two mega cities in India and dominant source region of secondary aerosols. *Atmos. Environ.* **146**, 90–99 (2016). <https://doi.org/10.1016/j.atmosenv.2016.06.069>
- Roy, A., Chatterjee, A., Tiwari, S., Sarkar, C., Das, S.K., Ghosh, S.K., Raha, S.: Precipitation chemistry over urban, rural and high altitude Himalayan stations in eastern India. *Atmos. Res.* **181**, 44–53 (2016). <https://doi.org/10.1016/j.atmosres.2016.06.005>
- Rozanski, K., Araguás-Araguás, L., Gonfiantini, R.: Isotopic Patterns in Modern Global Precipitation. *Journal of Geophysical Research Atmospheres.* 1–36 (1993). <https://doi.org/10.1029/GM078p0001>
- Sarin, M., Kumar, A., Srinivas, B., Sudheer, A.K., Rastogi, N.: Anthropogenic sulphate aerosols and large chloride deficit in marine atmospheric boundary layer of tropical bay of Bengal. *J. Atmos. Chem.* **66**(1–2), 1–10 (2010). <https://doi.org/10.1007/s10874-011-9188-z>
- Tian, L., Liu, Z., Gong, T., Yin, C., Yu, W., Yao, T.: Isotopic variation in the lake water balance at the Yamdrung-tso basin , southern Tibetan Plateau. *Hydrol. Process.* **22**, 3386–3392 (2008). <https://doi.org/10.1002/hyp>
- Tian, L., Masson-Delmotte, V., Stievenard, M., Yao, T., Jouzel, J.: Tibetan plateau summer monsoon northward extent revealed by measurements of water stable isotopes. *J Geophys Res Atmos.* **106**(D22), 28081–28088 (2001a). <https://doi.org/10.1029/2001JD900186>
- Tian, L., Yao, T., Numaguti, A., Sun, W.: Relation between stable isotope in monsoon precipitation in southern Tibetan Plateau and moisture transport history. *Science in China (Series D)*. **44**, (2001b). <https://doi.org/10.2151/jmsj.79.959>
- Tiwari, S., Chate, D.M., Bisht, D.S., Srivastava, M.K., Padmanabhamurty, B.: Rainwater chemistry in the North Western Himalayan Region, India. *Atmospheric Research.* 104–105, 128–138 (2012). <https://doi.org/10.1016/j.atmosres.2011.09.006>
- Tiwari, S., Hopke, P.K., Thimmaiah, D., Dumka, U.C., Srivastava, A.K., Bisht, D.S., Rao, P.S.P., Chate, D.M., Srivastava, M.K., Tripathi, S.N.: Nature and sources of ionic species in precipitation across the indo-Gangetic plains India. *Aerosol Air Qual Res.* **16**(4), 943–957 (2016). <https://doi.org/10.4209/aaqr.2015.06.0423>

- Tripathee, L., Kang, S., Rupakthetic, D., Cong, Z., Zhang, Q., Huang, J.: Chemical characteristics of soluble aerosols over the Central Himalayas : insights into spatiotemporal variations and sources. *Environ Sci Pollut Res.* **24**, 24454–24472 (2017). <https://doi.org/10.1007/s11356-017-0077-0>
- Tripathee, L., Kang, S., Huang, J., Sillanpää, M., Sharma, C.M., Lüthi, Z.L., Guo, J., Paudyal, R.: Ionic composition of wet precipitation over the southern slope of central Himalayas, Nepal. *Environmental Science and Pollution Research.* **21**(4), 2677–2687 (2014). <https://doi.org/10.1007/s11356-013-2197-5>
- Tripathee, L., Kang, S., Rupakheti, D., Zhang, Q., Huang, J., Sillanpää, M.: Water-soluble ionic composition of aerosols at urban location in the foothills of Himalaya, Pokhara Valley, Nepal. *Atmosphere.* **7**(8), (2016). <https://doi.org/10.3390/atmos7080102>
- Wang, L., Shen, Z., Lu, D., Xu, H., Zhang, N., Lei, Y., Cao, J.: Water-Soluble Ions and Oxygen Isotope in Precipitation over a Site in Northeastern Tibetan Plateau , China. *Journal of Atmospheric Chemistry.* (2019)
- Wu, D., Tie, X., Deng, X.: Chemical characterizations of soluble aerosols in southern China. *Chemosphere.* **64**(5), 749–757 (2006). <https://doi.org/10.1016/j.chemosphere.2005.11.066>
- Wu, Q., Han, G., Tao, F., Tang, Y.: Chemical composition of rainwater in a karstic agricultural area Southwest China: The impact of urbanization. *Atmos Res.* **111**, 71–78 (2012). <https://doi.org/10.1016/j.atmosres.2012.03.002>
- Xiao, J.: Chemical composition and source identification of rainwater constituents at an urban site in Xi'an. *Environ. Earth Sci.* **75**(3), 1–12 (2016). <https://doi.org/10.1007/s12665-015-4997-z>
- Xing, J., Song, J., Yuan, H., Li, X., Li, N., Duan, L., Xu, B., Wang, Q., Kang, X.: Chemical characteristics , deposition fluxes and source apportionment of precipitation components in the Jiaozhou Bay, North China. *Chemical characteristics , deposition fluxes and source apportionment of precipitation components in the Jiaozhou Bay North China. Atmos Res.* **190**, 10–20 (2017). <https://doi.org/10.1016/j.atmosres.2017.02.001>
- Yang, X., Yao, T., Yang, W., Xu, B., He, Y., Qu, D.: Isotopic signal of earlier summer monsoon onset in the bay of Bengal. *J. Clim.* **25**(7), 2509–2516 (2012). <https://doi.org/10.1175/JCLI-D-11-00180.1>
- Yao, T., Masson-delmotte, V., Gao, J., Yu, W., Yang, X., Risi, C., Sturm, C., Werner, M., Zhao, H., He, Y., Ren, W., Tian, L., Shi, C., Hou, S.: A review of climatic controls on $\delta^{18}\text{O}$ in precipitation over the Tibetan plateau : observations and simulations. *Rev. Geophys.* **52**, 525–548 (2013). <https://doi.org/10.1002/rog.20023.1>
- Yu, R., Xu, Y., Zhou, T., Li, J.: Relation between rainfall duration and diurnal variation in the warm season precipitation over central eastern China. *Geophys. Res. Lett.* **34**(13), 10–13 (2007a). <https://doi.org/10.1029/2007GL030315>
- Yu, W., Yao, T., Tian, L., Ma, Y., Ichiyonagi, K., Wang, Y., Sun, W.: Relationships between $\delta^{18}\text{O}$ in precipitation and air temperature and moisture origin on a south-north transect of the Tibetan plateau. *Atmos. Res.* **87**(2), 158–169 (2008). <https://doi.org/10.1016/j.atmosres.2007.08.004>
- Yu, W., Yao, T., Tian, L., Ma, Y., Kurita, N., Ichiyonagi, K., Wang, Y., Sun, W.: Stable isotope variations in precipitation and moisture trajectories on the Western Tibetan plateau, China. *Arctic, Antarctic, and Alpine Research.* **39**(4), 688–693 (2007b). [https://doi.org/10.1657/1523-0430\(07-511\)\[YU\]2.0.CO;2](https://doi.org/10.1657/1523-0430(07-511)[YU]2.0.CO;2)
- Yu, W., Yao, T., Tian, L., Ma, Y., Wen, R., Devkota, L. P., Wang, W., Qu, D., Chhetri, T. B.: Short-term variability in the dates of the Indian monsoon onset and retreat on the southern and northern slopes of the Central Himalayas as determined by precipitation stable isotopes. *Clim. Dyn.* **47**(1–2), 159–172 (2016). <https://doi.org/10.1007/s00382-015-2829-1>, 172
- Zhang, D.D., Peart, M.R., Jim, C.Y., La, J.: Alkaline rains on the Tibetan plateau and their implication for the original pH of natural rainfall. *J Geophys Res Atmos.* **107**(14), 1–6 (2002). <https://doi.org/10.1029/2001JD001332>
- Zhang, L., Qiao, B., Wang, H., Tian, M., Cui, J., Fu, C., Huang, Y., Yang, F.: Chemical characteristics of precipitation in a typical urban site of the hinterland in three gorges reservoir China. *J Chem.* (2018). <https://doi.org/10.1155/2018/2914313>
- Zhang, M., Wang, S., Wu, F., Yuan, X., Zhang, Y.: Chemical compositions of wet precipitation and anthropogenic influences at a developing urban site in southeastern China. *Atmos. Res.* **84**(4), 311–322 (2007). <https://doi.org/10.1016/j.atmosres.2006.09.003>
- Zhang, N., Cao, J., He, Y., Xiao, S.: Chemical composition of rainwater at Lijiang on the southeast Tibetan plateau : influences from various air mass sources. *J. Atmos. Chem.* **71**, 157–174 (2014). <https://doi.org/10.1007/s10874-014-9288-7>
- Zhang, Y., Kang, S., Li, C., Cong, Z., Zhang, Q.: Wet deposition of precipitation chemistry during 2005–2009 at a remote site (Nam co Station) in central Tibetan plateau. *J. Atmos. Chem.* **69**(3), 187–200 (2012). <https://doi.org/10.1007/s10874-012-9236-3>
- Zhao, P., Tan, L., Zhang, P., Wang, S., Cui, B., Li, D., Xue, G., Cheng, X.: Stable isotopic characteristics and influencing factors in precipitation in the monsoon marginal region of northern China. *Atmosphere.* **9**(97), 1–13 (2018). <https://doi.org/10.3390/atmos9030097>

Publisher's note Springer Nature remains neutral with regard to jurisdictional claims in published maps and institutional affiliations.

Affiliations

Subash Adhikari^{1,2,3,4} · **Fan Zhang**^{1,2,3} · **Chen Zeng**¹ · **Lekhendra Tripathee**^{5,6} · **Namita Paudel Adhikari**^{3,7} · **Jie Xu**^{1,3} · **Guanxing Wang**^{1,3}

✉ Fan Zhang
Zhangfan@itpcas.ac.cn

¹ Key Laboratory of Tibetan Environment Changes and Land Surface Processes, Chinese Academy of Sciences, Institute of Tibetan Plateau Research, Beijing, China

² CAS Center for Excellence in Tibetan Plateau Earth Sciences, Beijing, China

³ University of Chinese Academy of Sciences, Beijing, China

⁴ Janapriya Multiple Campus, Tribhuvan University, Pokhara 33700, Nepal

⁵ State Key Laboratory of Cryospheric Science, Chinese Academy of Sciences, Northwest Institute of Eco-Environment and Resources, Lanzhou 730000, China

⁶ Himalayan Environment Research Institute (HERI), Kathmandu, Nepal

⁷ Key Laboratory of Alpine Ecology and Biodiversity, Chinese Academy of Sciences, Institute of Tibetan Plateau Research, Beijing, China